JOURNAL OF THEORETICAL
AND APPLIED MECHANICS
3, 40, 2002

STATIC AND DYNAMIC ANALYSIS OF MULTILAYER COMPOSITE PLATE WITH PIEZOELECTRIC ELEMENTS

ZDZISŁAW MIESZCZAK[1)]
MAREK KRAWCZUK[1,2)]
WIESŁAW OSTACHOWICZ[1)]

[1)] *Institute of Fluid Flow Machinery, Polish Academy of Sciences, Gdańsk*

[2)] *University of Warmia and Mazury, Olsztyn*

e-mail: zdzislaw@imp.gda.pl; mk@imp.gda.pl; wieslaw@imp.gda.pl

In this paper a model of a composite, multi-layer plate with piezoelectric elements (PZT) has been presented. The influence of the stress stiffness matrix $\mathbf{K}_g$ on the results obtained has been shown. The model has been built up by making use of the finite element method (FEM). The issue of numerical calculations corroborated that the forces, which are formed as a result of activation of piezoelectric elements are considerable. These forces cause changes in static and dynamic characteristics of the element under consideration. The forces cause changes in displacements, stresses, natural frequencies and mode shapes as well. The changes in static characteristics are bigger than changes in dynamic one, moreover, the changes in the natural frequencies are bigger than those in mode shapes.

Key words: piezoelectric layer, composite plate, stress stiffness matrix, finite elements, active control

1. Introduction

Vibrations of machines are a serious problem. The level of vibrations can be reduced in various ways. Nevertheless, vibrations can not be eliminated fully. For this reason in many practical situations vibrations are controlled actively, in order to minimise their negative influence on the lifetime of machines. The level of vibrations can be greatly controlled by activation of PZT elements (Celentano and Setola, 1999; Hwang and Park, 1993; Tseng, 1989; Tzou and Ye, 1996).

Piezoelectric materials can be used in smart structures as sensors or actuators in applications such as shape control, active damping and acoustic noise

suppression. The design of such systems requires accurate electromechanical models to simulate the interaction between the structure and piezoelectric elements. The recent literature addresses the modelling of piezoelectric elements either bonded or embedded to several different types of structures.

Piezoelectric actuation of beams was treated in depth by Crawley and de Luis (1987), Cravley and Anderson (1990). Several other formulations were also presented for modelling of plates Keilers and Chang (1992), Ghosh and Batra (1995), Batra et al. (1996).

Deformation of plates may have significant influence on mechanical behaviour, affecting flexural stiffness and, hence, dynamic and stability characteristics of isotropic (Brunelle and Robertson, 1974) and laminated plates (Yang and Shieh, 1987). Rammerstorfer (1977) determined the optimum fields of residual in-plane stresses, which maximize the first natural frequency and buckling load of plates. Almeida and Hansen (1997) showed that, with a proper design, the in-plane thermal residual stresses from the curing process can be tailored to significantly enhance mechanical behaviour by increasing the critical buckling load of symmetric composite plates. Hernandes et al. (2000) investigated the problem of free vibration behaviour of composite plates equipped with surface piezoelectric elements, considering the stress stiffening effect.

In this work a model of a composite, multi-layer plate with piezoelectric outer layers is presented. The piezoelectric elements establish a part of the plate in this model. The finite element model has been used in order to analyse the influence of activation of the piezoelectric elements on changes in static and dynamic responses of the plate.

The purpose of this work is to investigate the complex problem of static and dynamic behaviour of composite plates equipped with surface bonded piezoelectric elements, considering the stress stiffening effect caused by the in-plane-induced deformation. With this in mind, non-linear strain-displacement relations are used to formulate a finite element model including the geometric stiffness associated with the in-plane piezoelectric-induced stress. Several examples illustrate how the induced stress stiffening influences the static and dynamic behaviour of simply-supported square plates equipped with the piezoelectric patches.

2. Finite element model of the plate

The plate was modelled by plate finite elements with eight nodes. Each node has five mechanical degrees of freedom (longitudinal u^0, v^0 displacement,

transverse displacement w, independent rotation φ_x^0, φ_y^0). Scheme of the plate finite element is presented in Fig. 1. Similarly, the PZT layers are modelled by plate finite elements with eight nodes but each node has six degrees of freedom – five mechanical and one electrical (longitudinal u^0, v^0 displacement, transverse displacement w^0, independent rotation φ_x^0, φ_y^0 and one electrical degree of freedom modelling the potential function φ^0). Constitutive equations of piezoelectric materials are included in Appendix.

The model does not take into account the damping effects.

The displacements u, v, w in the plate are given by the following equations (Vinson and Sierakowski, 1989)

$$\begin{aligned} u(x,y,z) &= u^0(x,y) + z\varphi_x^0(x,y) \\ v(x,y,z) &= v^0(x,y) + z\varphi_y^0(x,y) \\ w(x,y,z) &= w^0(x,y) \end{aligned} \tag{2.1}$$

whereas the electric field ϕ of the plate piezoelectric element is described by using the polynomials ϕ^0 (Tzou and Ye, 1996)

$$\phi(x,y,z) = z\phi^0(x,y) \tag{2.2}$$

We have assumed that the electric field is linearly distributed through thickness of the plate (for the thin plate).

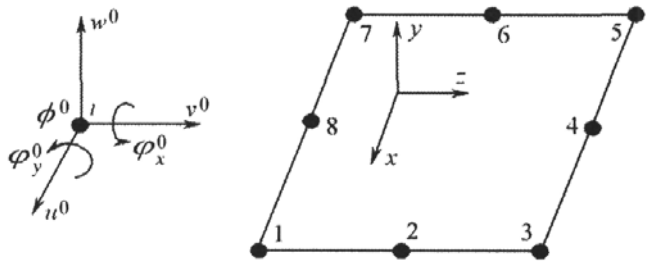

Fig. 1. Degrees of freedom of the piezoelectric plate finite element

The displacement field is approximated by the following polynomials according to Tessler and Dong (1981)

$$\begin{aligned} u^0 &= a_1 + a_2x + a_3y + a_4x^2 + a_5xy + a_6y^2 + a_7x^2y + a_8xy^2 \\ v^0 &= a_9 + a_{10}x + a_{11}y + a_{12}x^2 + a_{13}xy + a_{14}y^2 + a_{15}x^2y + a_{16}xy^2 \\ w^0 &= a_{17} + a_{18}x + a_{19}y + a_{20}x^2 + a_{21}xy + a_{22}y^2 + a_{23}x^2y + a_{24}xy^2 \end{aligned} \tag{2.3}$$

$$\begin{aligned}
\varphi_x^0 &= a_{25} + a_{26}x + a_{27}y + a_{28}x^2 + a_{29}xy + a_{30}y^2 + a_{31}x^2y + a_{32}xy^2 \\
\varphi_y^0 &= a_{33} + a_{34}x + a_{35}y + a_{36}x^2 + a_{37}xy + a_{38}y^2 + a_{39}x^2y + a_{40}xy^2 \\
\phi^0 &= a_{41} + a_{42}x + a_{43}y + a_{44}x^2 + a_{45}xy + a_{46}y^2 + a_{47}x^2y + a_{48}xy^2
\end{aligned} \tag{2.4}$$

The constants $a_1 \div a_{48}$ are expressed by nodal displacements using the element boundary conditions. When the constants $a_1 \div a_{48}$ are known, the shape functions matrix **N** is determined. The strains can be expressed as follows (Ghosh and Batra, 1995)

$$\begin{aligned}
&\varepsilon_x = \frac{\partial u}{\partial x} && \varepsilon_y = \frac{\partial v}{\partial y} \\
&\gamma_{xy} = \frac{\partial u}{\partial y} + \frac{\partial v}{\partial x} && \gamma_{yz} = \frac{\partial v}{\partial z} + \frac{\partial w}{\partial y} && \gamma_{xz} = \frac{\partial u}{\partial z} + \frac{\partial w}{\partial x} \\
&\varepsilon_{\phi x} = \frac{\partial \phi}{\partial x} && \varepsilon_{\phi y} = \frac{\partial \phi}{\partial y}
\end{aligned} \tag{2.5}$$

where

$\varepsilon_x, \varepsilon_y$	–	normal strain parallel to x and y axis
$\gamma_{xy}, \gamma_{yz}, \gamma_{xz}$	–	shear strain tangent to xy, yz, xz plane
$\varepsilon_{\phi x}, \varepsilon_{\phi y}$	–	normal strain derived to the voltage V and parallel to x and y axis.

Using the standard finite element, the matrix of relationships between the strains and nodal displacements **B** can be obtained.

The matrix of elasticity coefficients **D** for the PZT layer has the following form (Tseng, 1989)

$$\mathbf{D} = \begin{bmatrix}
s_{11} & s_{12} & 0 & 0 & 0 & 0 & 0 \\
s_{12} & s_{22} & 0 & 0 & 0 & 0 & 0 \\
0 & 0 & s_{66} & 0 & 0 & 0 & 0 \\
0 & 0 & 0 & s_{44} & 0 & 0 & e_{24} \\
0 & 0 & 0 & 0 & s_{55} & e_{15} & 0 \\
0 & 0 & 0 & 0 & e_{15} & \varepsilon_{11} & 0 \\
0 & 0 & 0 & e_{24} & 0 & 0 & \varepsilon_{22}
\end{bmatrix} \tag{2.6}$$

where the expressions s_{11}, s_{12}, s_{22}, s_{44}, s_{55}, s_{66} are calculated from (Vinson and Sierakowski, 1989)

$$\begin{aligned}
s_{11} &= s_{22} = s_{66} = \widetilde{s}_{11}\cos^4\alpha + 2(\widetilde{s}_{12} + 2\widetilde{s}_{66})\sin^2\alpha\cos^2\alpha + \widetilde{s}_{22}\sin^2\alpha \\
s_{12} &= (\widetilde{s}_{11} + \widetilde{s}_{22} - 4\widetilde{s}_{66})\sin^2\alpha\cos^2\alpha + \widetilde{s}_{12}(\sin^4\alpha + \cos^4\alpha) \\
s_{44} &= \widetilde{s}_{44}\cos^2\alpha + \widetilde{s}_{55}\sin^2\alpha \\
s_{55} &= \widetilde{s}_{44}\sin\alpha^2 + \widetilde{s}_{55}\cos^2\alpha
\end{aligned} \tag{2.7}$$

while

$$\widetilde{s}_{11} = \frac{E_{11}}{1 - \nu_{12}^2 \frac{E_{22}}{E_{11}}} \qquad \widetilde{s}_{22} = \frac{E_{22}}{1 - \nu_{12}^2 \frac{E_{22}}{E_{11}}} \qquad \widetilde{s}_{12} = \frac{\nu_{12} E_{11}}{1 - \nu_{12}^2 \frac{E_{22}}{E_{11}}}$$
$$\widetilde{s}_{44} = \frac{G_{23}}{2} \qquad \widetilde{s}_{55} = \frac{G_{12}}{2} \qquad \widetilde{s}_{66} = \frac{G_{22}}{2} \tag{2.8}$$

where

α – angle between the x-axes and direction of fibres location
e_{15}, e_{24} – means the piezoelectric shearing stress constants
$\varepsilon_{11}, \varepsilon_{22}$ – dielectric permittivities – see Appendix.

The stiffness matrix $\mathbf{K}$ is calculated as

$$\mathbf{K} = \sum_{n=1}^{N} \int_V \mathbf{B}^\top \mathbf{D} \mathbf{B} \, dV \tag{2.9}$$

where $\mathbf{B}$ is the matrix of relationships between the strains and nodal displacements, and $\mathbf{D}$ is the matrix of elasticity coefficients.

Finally, the stiffness matrix can be presented as

$$\mathbf{K} = \begin{bmatrix} \mathbf{K}_{mm} & \mathbf{K}_{me} \\ \mathbf{K}_{me} & \mathbf{K}_{ee} \end{bmatrix} \tag{2.10}$$

where $\mathbf{K}_{mm}$ denotes the mechanical part of the stiffness matrix, $\mathbf{K}_{me}$ is the electromechanical part of this matrix and $\mathbf{K}_{ee}$ express the electrical part of the stiffness matrix of the PZT layer.

The inertia matrix $\mathbf{M}$ is calculated as

$$\mathbf{M} = \int_V \rho \mathbf{N}^\top \mathbf{N} \, dV \tag{2.11}$$

where $\mathbf{N}$ is the shape function matrix and ρ denotes density.

The stress stiffness matrix $\mathbf{K}_g$ is given by Bossak (1977)

$$\mathbf{K}_g = \int_V \mathbf{G}^\top \mathbf{S} \mathbf{G} \, dV \tag{2.12}$$

where $\mathbf{G}$ is expressed as follows

$$\mathbf{G} = [\mathbf{G}_i, \mathbf{G}_j, \mathbf{G}_n] \tag{2.13}$$

The matrix $\mathbf{G}_i$ is given

$$\mathbf{G}_i = \left[\frac{\partial N_i}{\partial x}\mathbf{I}_3, \frac{\partial N_i}{\partial x}\mathbf{I}_3, \frac{\partial N_i}{\partial x}\mathbf{I}_3\right] \tag{2.14}$$

where $\mathbf{I}_3$ denotes the 3×3 unit matrix and

$$\mathbf{S} = \begin{bmatrix} \sigma_x\mathbf{I}_3 & \tau_{yx}\mathbf{I}_3 & \tau_{xz}\mathbf{I}_3 \\ \tau_{yx}\mathbf{I}_3 & \sigma_y\mathbf{I}_3 & \tau_{yz}\mathbf{I}_3 \\ \tau_{xz}\mathbf{I}_3 & \tau_{yz}\mathbf{I}_3 & 0 \end{bmatrix} \tag{2.15}$$

while

σ_x, σ_y – normal stresses within the plate
$\tau_{yx}, \tau_{xz}, \tau_{yz}$ – shear stresses within the plate.

The matrix $\mathbf{K}_g$ depends on stresses (2.15). In turn, the stress depends on the load forces q and piezoelectric actuation.

3. Equation of motion and solution

The solution to equation of motion consists of two parts. Firstly, a linear equation of motion is solved. The equation of motion (without damping) of the analysed plate can be presented, in a general form, as follows (Muller, 1999)

$$\mathbf{M}\ddot{\boldsymbol{q}} + \mathbf{K}_{mm}\boldsymbol{q} = -\mathbf{K}_{me}\boldsymbol{U} + \boldsymbol{F}_m \tag{3.1}$$

where

$\boldsymbol{U}$ – vector of voltage
$\ddot{\boldsymbol{q}}$ – vector of nodal accelerations
$\boldsymbol{q}$ – vector of nodal displacements
$\boldsymbol{F}_m$ – mechanical force vector.

In the first step, the displacements and stresses within the plate are calculated. Having them found one derives stiffness matrix $\mathbf{K}_g$ of additional stresses.

In the second step, equation of motion (3.2), which includes $\mathbf{K}_g$, is solved

$$\mathbf{M}\ddot{\boldsymbol{q}} + (\mathbf{K}_{mm} + \mathbf{K}_g)\boldsymbol{q} = -\mathbf{K}_{me}\boldsymbol{U} + \boldsymbol{F}_m \tag{3.2}$$

Equation of motion (3.2) is solved in an iterative process. Completion of this process enables calculation of the natural frequencies from the following equation

$$\det[(\mathbf{K}_{mm} + \mathbf{K}_g) - \omega^2\mathbf{M}] = 0 \tag{3.3}$$

Results for the analysed plate are calculated following the algorithm shown in Fig. 2. The iterative process consists of several steps. The number of steps depends on mechanical load and forces which are generated as a result of activation of piezoelectric elements. The calculation finishes when 0.5% accuracy of the iterative process is achieved.

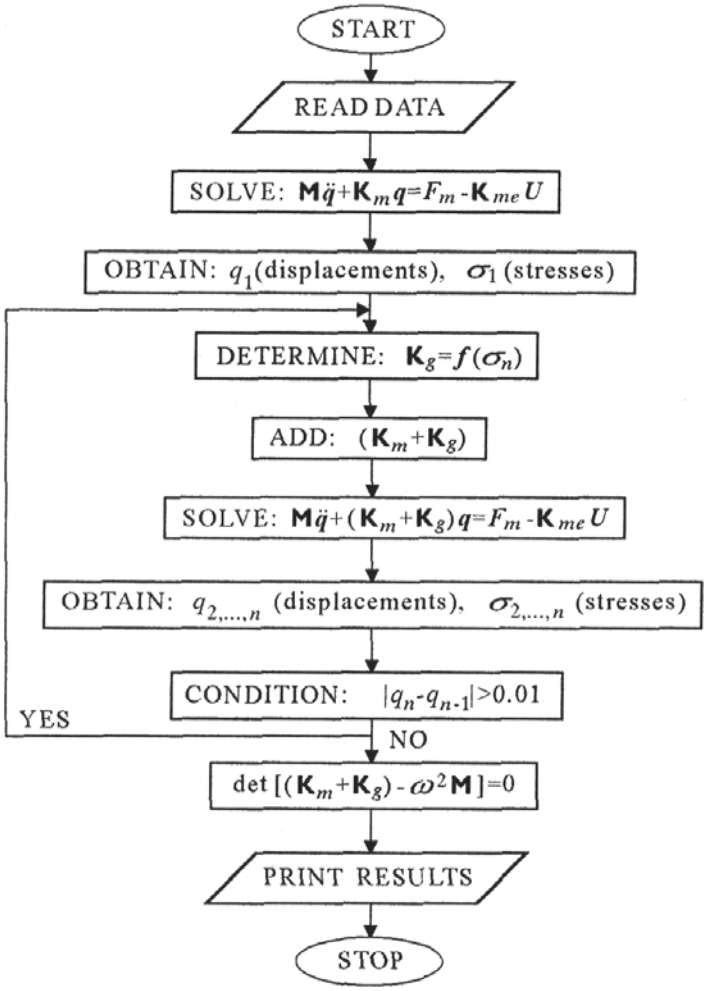

Fig. 2. Algorithm of the iterative process for solving the equation of motion

4. Numerical calculations

The analysed multilayer, simply-supported composite plate is presented in Fig. 3. Each layer is modelled by sixty four finite elements. Dimensions of the plate are: length and width $A = 250\,\text{mm}$, height $H = 1.0\,\text{mm}$,

$H_1 = 0.1$ mm. The graphite-epoxy laminate is anti-symmetric $[-\alpha/\alpha/-\alpha/\alpha]$ with $\alpha = 45°$. Properties of the graphite-epoxy T300/976 are: Young's modulus: $E_{11} = 150$ GPa, $E_{22} = E_{33} = 9$ GPa; shear modulus: $G_{23} = 2.5$ GPa, $G_{12} = G_{13} = 7.1$ GPa; Poisson's ratio: $\nu_{12} = \nu_{13} = \nu_{23} = 0.3$; density: $\rho = 1600\,\mathrm{kg/m^3}$. Properties of the PZT G1195N are: Young's modulus: $E_{11} = E_{22} = E_{33} = 63$ GPa; shear modulus: $G_{21} = G_{12} = G_{13} = 24.2$ Gpa; Poisson's ratio: $\nu_{12} = \nu_{13} = \nu_{23} = 0.3$; density: $\rho = 7600\,\mathrm{kg/m^3}$; piezoelectric constants: $e_{15} = e_{24} = 22.86\,\mathrm{c/m^2}$; dielectric permittivities: $\varepsilon_{11} = \varepsilon_{22} = 15.3 \cdot 10^{-9}$ GPa – see Rinat and Bar-Yoseph (2000).

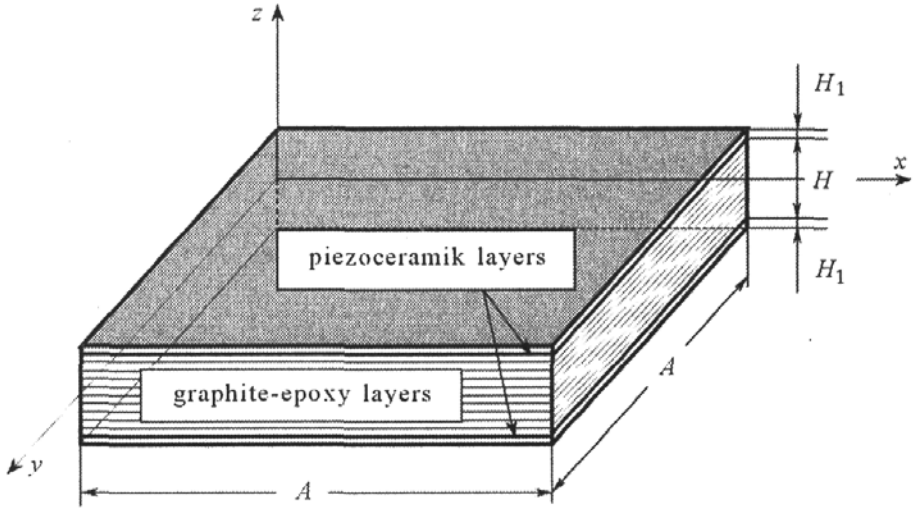

Fig. 3. Geometry of the piezoceramic anti-symmetric simply-supported composite plate

The plate is subjected to a uniformly distributed, mechanical, transverse load of $q = 1000\,\mathrm{N/m^2}$. Equal electric fields, but with an opposite sign, are applied across the thickness of the upper and lower piezoelectric layers, respectively. Due to the converse piezoelectric effect, strain is induced. The poling direction coincides with the z co-ordinate. The strain causes the upper piezoelectric layer to contract and the lower piezoelectric layer to expand.

4.1. Static analysis

In Fig. 4 the deflection of the plate according to the nonlinear theory, for a mechanical, transverse load of $q = 1000\,\mathrm{N/m^2}$ $(U = 0\,\mathrm{V})$ only, and for five active voltages $(U = 30,\ 60,\ 100,\ 130,\ 150\,\mathrm{V})$ and the same mechanical load are shown

The left picture in Fig. 4a shows the deflection of the plate for the mechanical, transverse load $(q = 1000\,\mathrm{N/m^2},\ U = 0\,\mathrm{V})$ only. Such a load causes

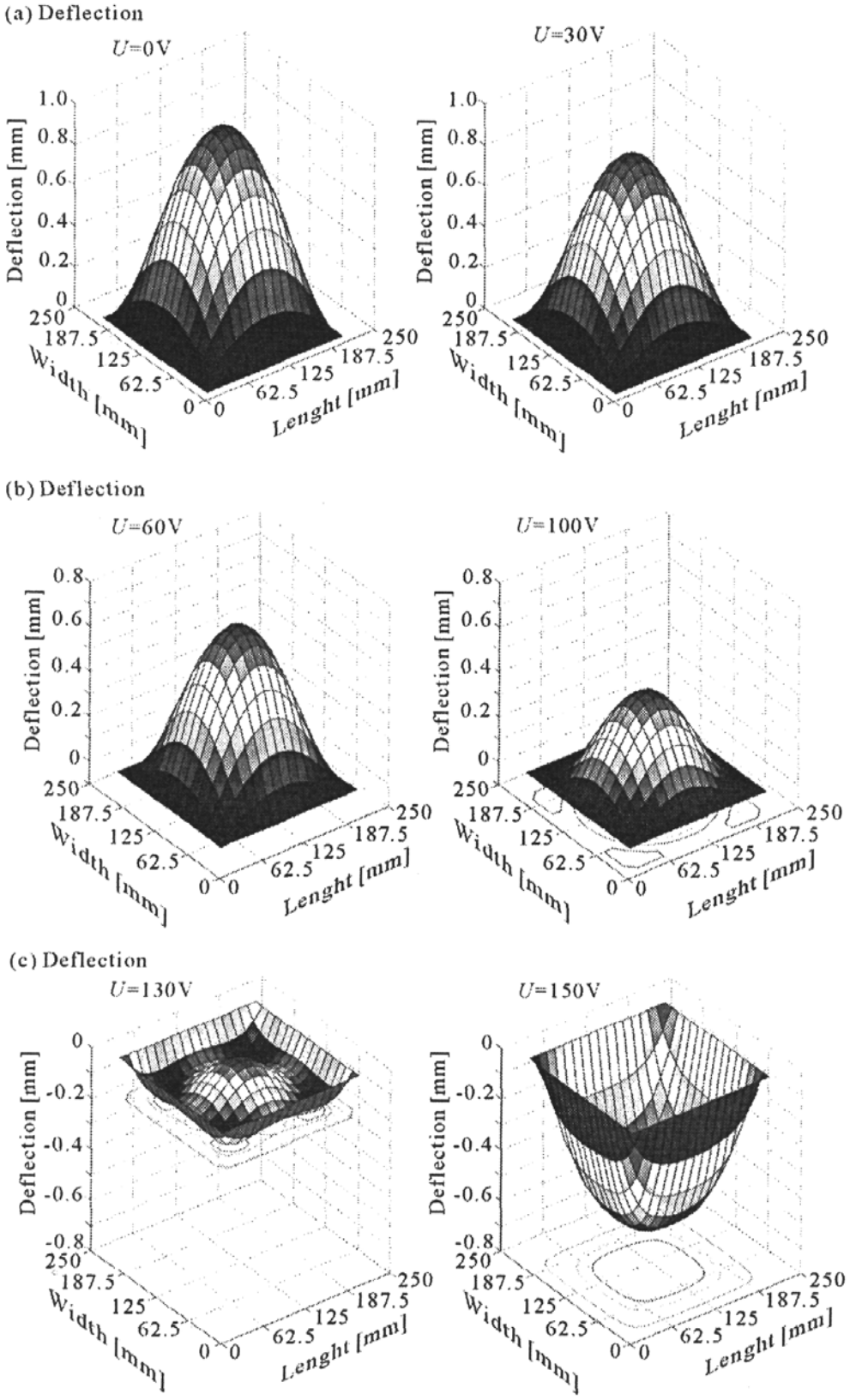

Fig. 4. Deflection due to a uniform transverse load and different actuators input voltage ($U = 0$, 30, 60, 100, 130, 150 V) – nonlinear model

the biggest deflection of the plate. The next pictures show that the changes in the deflection of the analysed plate depend on the actuators input voltage. The forces which are generated as a result of activation of the piezoelectric elements are considerable. The deflection of the central point is negative for the applied voltage $U = 150\,\mathrm{V}$ – see Fig. 4c.

In Table 1 deflections of the central point, according to the linear and nonlinear theories, for different actuators input voltages are compared. The differences between the linear and nonlinear computation are the biggest for the biggest strains (the matrix $\mathbf{K}_g$ is maximum for the maximum stresses).

Table 1. Central point deflection due to a uniform load and different actuators voltages

Central deflection q [mm]			
Input voltage [V]	Linear computation	Nonlinear computation – consideration $\mathbf{K}_g$	Number of iterations
0	1.312	0.978	5
30	1.035	0.850	4
60	0.759	0.687	4
100	0.391	0.399	4
130	0.115	0.193	4
150	−0.0685	−0.592	3

4.2. Dynamic analysis

Results of the dynamic analysis are presented in Fig. 5 and Fig. 6. The pictures show the influence of voltage U on changes in first eight natural frequencies of the analysed plate. For example, it is clearly shown in Fig. 5 that drop in the first natural frequency can reach almost 100%.

In Table 2 changes of the natural frequencies are compared. The relative changes in the natural frequencies of the analysed plate are the biggest for the lowest natural frequencies.

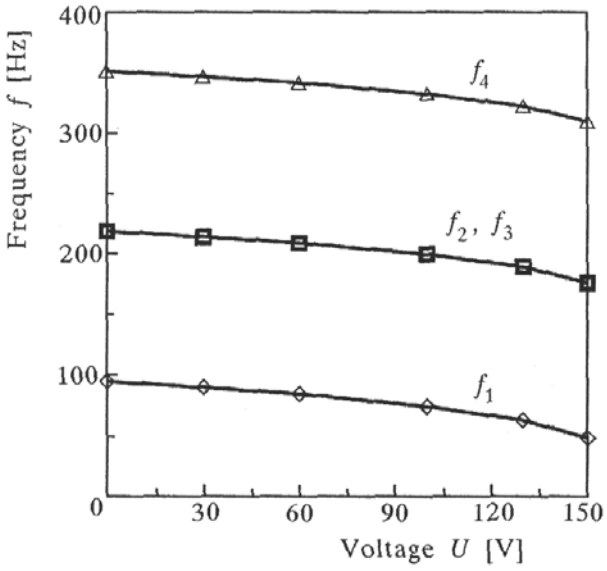

Fig. 5. Four first natural frequencies and their changes as a function of voltage

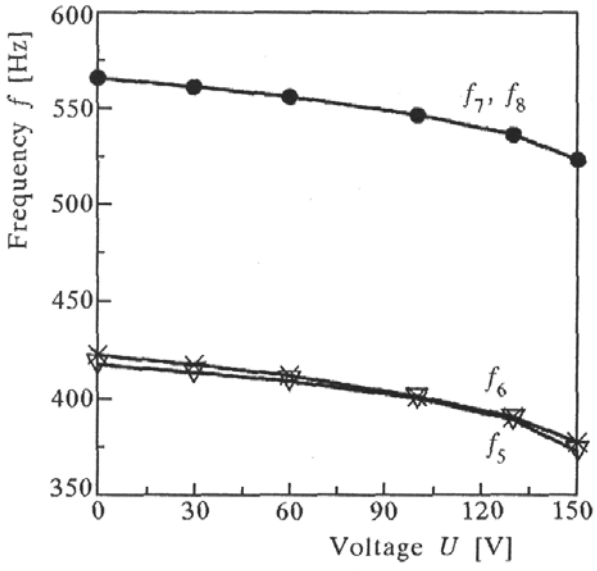

Fig. 6. Natural frequencies and their changes as a function of voltage

Table 2. Natural frequencies and their changes as a function of voltage

U [V]	Natural frequencies f [Hz]					
	f_1	f_2, f_3	F_4	f_5	f_6	f_7, f_8
0	94.57	218.6	351.7	417.4	422.3	565.7
30	89.77	214.1	347.1	413.3	417.3	561.0
f_{n0}/f_n [%]	5.34	2.14	1.32	0.99	1.19	0.83
60	84.37	209.1	342.1	408.9	411.8	556.0
f_{n0}/f_n [%]	12.08	4.54	2.80	2.07	2.54	1.74
100	74.15	199.7	332.7	400.0	400.9	546.3
f_{n0}/f_n [%]	27.53	9.46	5.71	4.35	5.33	3.55
130	62.91	189.5	322.7	388.8	390.3	536.1
f_{n0}/f_n [%]	50.32	15.35	8.98	7.35	8.19	5.52
150	48.33	176.0	310.1	372.5	377.2	523.0
f_{n0}/f_n [%]	95.67	24.20	13.41	12.05	11.95	8.16

Changes in the first six mode shapes of the plate according to the nonlinear theory, for a mechanical, transverse load of $q = 1000\,\mathrm{N/m^2}$ and for the same mechanical transverse load and active voltages ($U = 150\,\mathrm{V}$) are shown in Fig. 7 and Fig. 8. It can be noticed that the applied voltage brings about that the fifth and sixth mode shapes change their succession (see Fig. 8b,c).

Although the forces which are formed as a result of activation of the piezoelectric elements are considerable, the changes in the mode shapes are not significant. The differences between the mode shapes are practically invisible, at least for the presented example.

5. *Conclusion*

The elaborated element can be applied for static and dynamic analysis of plate-like structures with piezoelectric layers. The model has been successfully employed to the investigation of the influence of activation of the piezoelectric layers on changes in the static and dynamic characteristics of a simply-supported plate. Numerical examples presented in this paper allow the following conclusions to be drawn

- Stiffness matrix $\mathbf{K}_g$ of additional stresses influences the results significantly

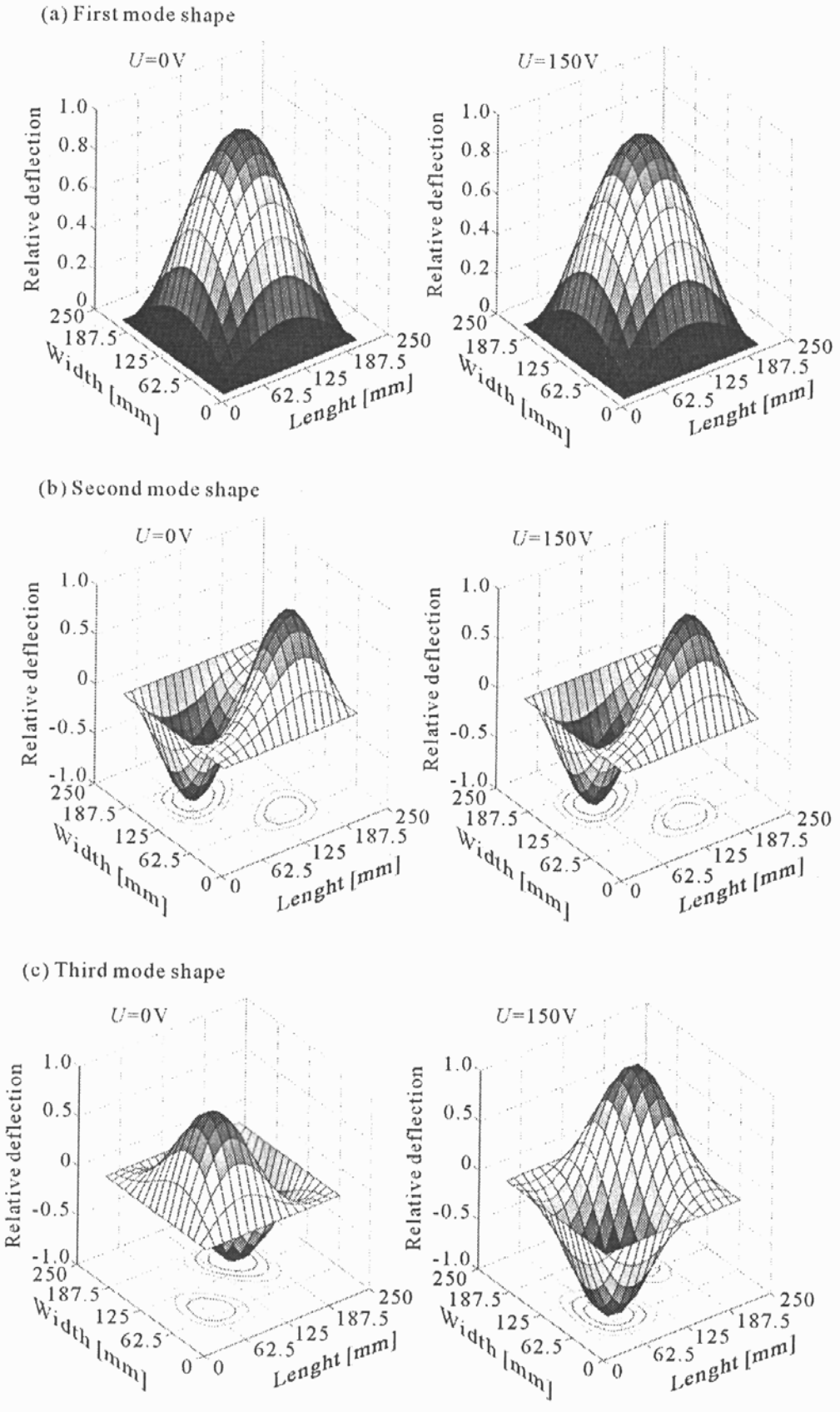

Fig. 7. Mode shapes of the plate for $U = 0\,\mathrm{V}$ and $U = 150\,\mathrm{V}$

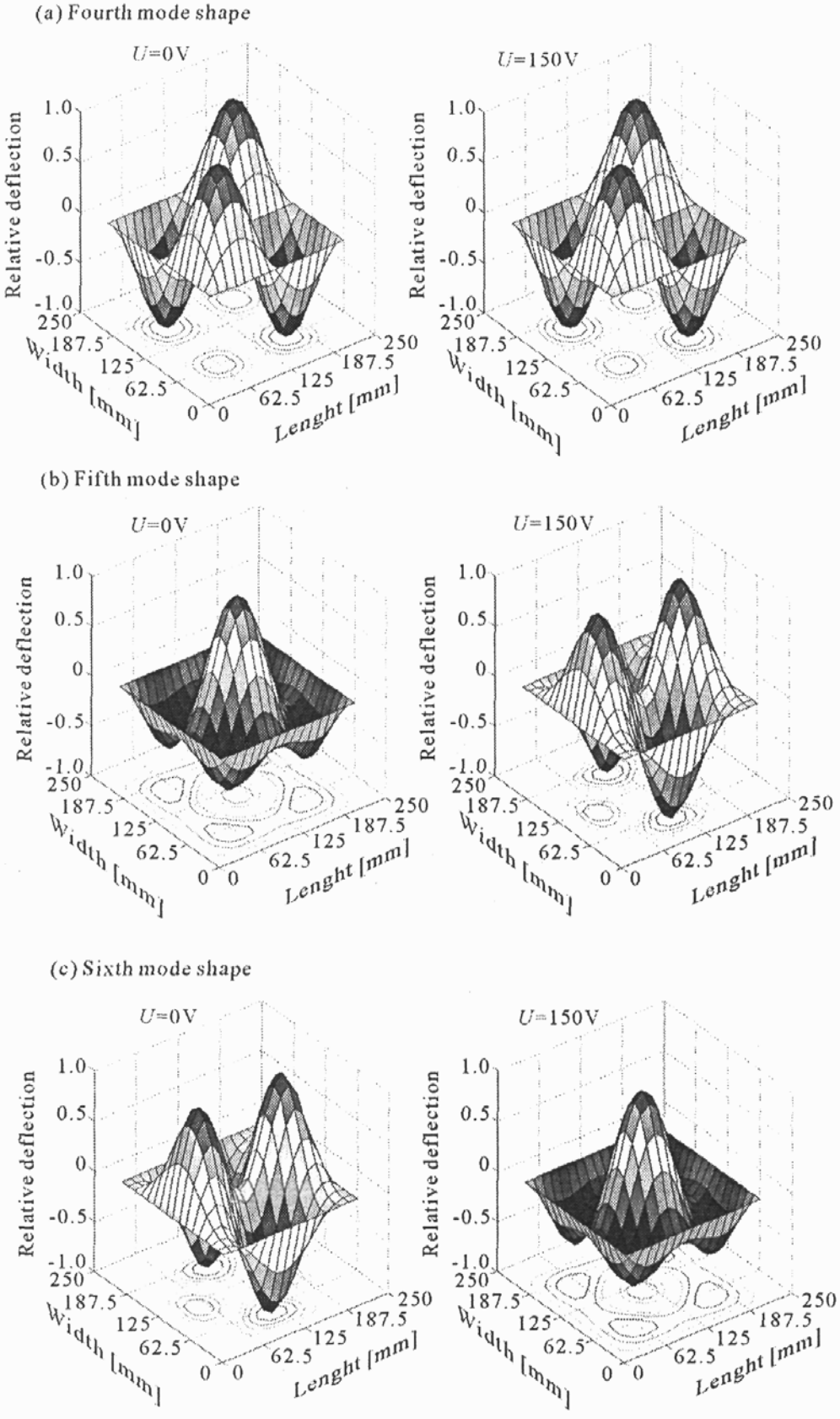

Fig. 8. Mode shapes of the plate for $U = 0\,\mathrm{V}$ and $U = 150\,\mathrm{V}$

- Relative changes in the static characteristics are bigger than those in the dynamic ones.
- Changes in the natural frequencies of the analysed plate are a function of the applied voltage.
- Forces which are generated as a result of activation of the piezoelectric elements are considerable. They influence changes in the natural frequencies significantly.
- Relative changes in the natural frequencies of the analysed plate are the biggest for the lowest natural frequency.

Using the method described in the paper it is possible to elaborate other types of elements made of composite layers and PZT elements.

A. Appendix

The linear constitutive equations of a piezoelectric composite plate can be written as (Sarawanos et al., 1997; Rinat and Bar-Yoseph, 2000)

$$\begin{aligned} \boldsymbol{\sigma}_i &= \mathbf{C}_{ij}\boldsymbol{\varepsilon}_j - \mathbf{e}_{ki}\boldsymbol{E}_k \\ \boldsymbol{D}_l &= \mathbf{e}_{lj}\boldsymbol{\varepsilon}_j - \mathbf{k}^{\varepsilon}_{lk}\boldsymbol{E}_k \end{aligned} \tag{A.1}$$

where $i, j = 1, 2, ..., 5$, $l, k = 1, 2$, and

- $\boldsymbol{\sigma}_i$ – stress vector
- $\boldsymbol{\varepsilon}_j$ – strain vector
- $\boldsymbol{E}_k$ – electric field vector
- $\boldsymbol{D}_l$ – electric displacement vector
- $\mathbf{C}_{ij}$ – elastic stiffness matrix
- $\mathbf{e}_{ik}$ – piezoelectric stress/charge tensor
- $\mathbf{k}^{\varepsilon}_{lk}$ – piezoelectric permittivity matrix.

For the piezoelectric material $\mathbf{e}_{ik}$ and $\mathbf{k}^{\varepsilon}_{lk}$ are given by

$$\mathbf{e}_{ik} = \begin{bmatrix} 0 & 0 & 0 & 0 & e_{15} & 0 \\ 0 & 0 & 0 & e_{24} & 0 & 0 \\ e_{31} & e_{32} & e_{33} & 0 & 0 & 0 \end{bmatrix} \qquad \mathbf{k}^{\varepsilon}_{lk} = \begin{bmatrix} k_{11}0 & 0 & \\ 0 & k_{22} & 0 \\ 0 & 0 & k_{33} \end{bmatrix} \tag{A.2}$$

where

- e_{31}, e_{32}, e_{33} – piezoelectric stress constants
- e_{15}, e_{24} – piezoelectric shearing stress constants.

References

1. ALMEIDA S.F.M., HANSEN J.S., 1977, Enhanced elastic buckling loads of composite plates with tailored thermal residual stresses, *Journal Appl. Mech.*, **64**, 4, 772-780

2. BATRA R.C., LIANG X.Q., YANG J.S., 1996, Shape control of vibrating simply supported rectangular plates, *AIAA Journal*, **34**, 1, 116-122

3. BOSSAK M., 1977, *Dynamika Układów Wstępnie Obciążonych*, Wydawnictwo Uczelniane Politechniki Rzeszowskiej im. Ignacego Łukasiewicza, Rzeszów

4. BRUNELLE E.J., ROBERTSON S.R., 1974, Initially stressed mindlin plates, *AIAA Journal*, **12**, 8, 1036-1045

5. CELENTANO G., SETOLA R., 1999, The modelling of a flexible beam with piezoelectric plates for active vibration control, *Journal of Sound and Vibration*, **223**, 483-492

6. CRAWLEY E., ANDERSON E., 1990, Detailed models of piezoelectric actuation of beams, *Journal of Intell. Mater. Syst. Struc.*, **1**, 1, 4-25

7. CRAWLEY E., DE LUIS J., 1987, Use of the piezoelectric actuators as elements of intelligent structures, *AIAA Journal*, **25**, 10, 1373-1385

8. GHOSH K., BATRA R.C., 1995, Shape control of plates using piezoceramic elements, *AIAA Journal*, **33**, 7, 1354-1357

9. HERNANDES J.A., MULLER DE ALMEIDA S.F., NABARRETE A., 2000, Stiffening effects on the free vibration behaviour of composite plates with PZT actuators, *Composite Structures Journal*, **37**, 8, 1017-1019

10. HWANG W-S., PARK C.H., 1993, Finite element modeling of piezoelectric sensors and actuators, *AIAA Journal*, **31**, 5, 930-937

11. MULLER DE ALMEIDA S.F., 1999, Shape control of laminated plates with piezoelectric actuators including stress-stiffening effects, *AIAA Journal*, **37**, 8, 1017-1019

12. RAMMERSTORFER F.G., 1977, Increase of the first natural frequency and buckling load of plates by optimal fields of initial stresses, *Acta Mech.*, **27**, 1-4, 217-238

13. RINAT Y., BAR-YOSEPH P.Z., 2000, Space-time special elements for nonlinear static and dynamics modelling of piezoelectric composite laminated plates, *Proc. ECCOMAS 2000*, Barcelona, 1-20

14. SARAWANOS D., HEYLIGER P., HOPKINS D., 1997, Layerwise mechanics and finite element for the dynamic analysis of piezoelectric composite plates, *Journal of Solid and Structures*, **34**, 3, 359-378

15. TSENG, C.-I., 1989, Electromechanical dynamics of a coupled piezoelectric/mechanical system applied to vibration control and distributed sensing, Pd.D. Thesis, Univ. of Kentucky, Lexington

16. TZOU H., TSENG C., 1990, Distributed piezoelectric sensor/actuator design for dynamic measurement/control of distributed parameter systems: a piezoelectric finite element approach, *Journal of Sound and Vibration*, **138**, 1, 17-34

17. TZOU H.S., YE R., 1996, Analysis of piezoelectric structures with laminated piezoelectric triangle shell elements, *AIAA Journal*, **34**, 1, 110-115

18. TESSLER A., DONG S.B., 1981, On a hierarchy of conforming Timoshenko beam elements, *Computer and Structure*, **38**, 334-344

19. VINSON J.R., SIERAKOWSKI R.L., 1989, *Behaviour of Structures Composed of Composite Materials*, Martinus Nijhoff, Dorchester

20. YANG I.H., SHIEH J.A., 1987, Vibrations of initially stressed thick rectangular orthotropic plates, *Journal of Sound and Vibration*, **119**, 3, 545-558

Statyka i dynamika wielowarstwowych płyt kompozytowych z elementami piezoelektrycznymi

Streszczenie

W pracy przedstawiono model kompozytowej płyty wielowarstwowej z aktywnymi elementami piezoelektrycznymi (PZT). Model zbudowano w oparciu o metodę elementów skończonych (MES). W pracy pokazano wpływ macierzy sztywności naprężeń początkowych $\mathbf{K}_g$ na otrzymywane charakterystyki statyczne i dynamiczne analizowanej płyty. Wyniki symulacji numerycznych wykazały, że siły powstałe w efekcie aktywacji elementów piezoelektrycznych są znaczne i powodują zmiany w charakterystykach statycznych i dynamicznych całej konstrukcji; wpływają na wartości przemieszczeń, naprężeń, częstości oraz postaci drgań własnych. Badania numeryczne wykazały, że aktywne elementy piezoelektryczne powodują większe zmiany charakterystyk statycznych niż dynamicznych. Z kolei, uwzględnienie w modelu sztywności naprężeń początkowych w większym stopniu wpływa na zmianę częstości drgań własnych, niż na zmianę postaci drgań własnych.

Manuscript received January 15, 2002; accepted for print March 4, 2002